PHYSICAL REVIEW A **92**, 031403(R) (2015)

Ultra-long-range Rydberg molecules in a divalent atomic system

B. J. DeSalvo,[1] J. A. Aman,[1] F. B. Dunning,[1] T. C. Killian,[1,*] H. R. Sadeghpour,[2] S. Yoshida,[3] and J. Burgdörfer[3]

[1]*Department of Physics and Astronomy, Rice University, Houston, Texas 77251, USA*

[2]*ITAMP, Harvard-Smithsonian Center for Astrophysics, 60 Garden Street, Cambridge, Massachusetts 02138, USA*

[3]*Institute for Theoretical Physics, Vienna University of Technology, Vienna, Austria, EU*

(Received 26 March 2015; published 28 September 2015)

We report the creation of ultra-long-range Sr_2 molecules comprising one ground-state $5s^2\ ^1S_0$ atom and one atom in a $5sns\ ^3S_1$ Rydberg state for n ranging from 29 to 36. Molecules are created in a trapped ultracold atomic gas using two-photon excitation near resonant with the $5s5p\ ^3P_1$ intermediate state, and their formation is detected through ground-state atom loss from the trap. The observed molecular binding energies are reproduced with the aid of first-order perturbation theory that utilizes a Fermi pseudopotential with effective s-wave and p-wave scattering lengths to describe the interaction between an excited Rydberg electron and a ground-state Sr atom.

DOI: 10.1103/PhysRevA.92.031403 PACS number(s): 33.80.Rv, 32.80.Ee, 34.20.Cf

Low-energy scattering of the nearly free, excited electron in a Rydberg atom from a ground-state atom can bind the two atoms into an ultra-long-range Rydberg molecule [1,2]. The resulting internuclear spacing is of the order of the size of the Rydberg atom, which scales with the principal quantum number, n, as n^2 and can exceed 1 μm. This class of molecules has attracted significant attention because it demonstrates a new mechanism for chemical bonding and the molecules possess surprising features, such as the presence of a permanent electric dipole moment, even in the homonuclear case [3]. Here, we report the creation and theoretical description of ultra-long-range Sr_2 molecules involving a $5sns\ ^3S_1$ Rydberg atom.

Ultra-long-range molecules were originally predicted theoretically [1] and were subsequently observed in Rb [2] and Cs [4]. The original observations were of dimers involving spherically symmetric S Rydberg states [2], but now measurements have been extended to anisotropic P [5,6] and D [7,8] Rydberg states and to molecules comprising one Rydberg atom and as many as four ground-state atoms [9]. Excitation of Rb(nD) [9] and Cs(nP) [6] Rydberg molecules has revealed considerable spectral complexity due to the Rydberg electron spin-orbit and ground-state hyperfine interactions, which results in mixing of singlet and triplet electronic symmetries. For bosonic alkaline-earth metal atoms, such as ^{84}Sr studied here, both these interactions are absent. In addition, scattering of electrons from ground-state Rb and Cs atoms displays a low-energy resonance that further complicates the molecular structure and greatly reduces the lifetime of Rydberg molecules [10] and Rydberg atoms in a dense gas [11] in these systems. ^{84}Sr does not possess a p-wave resonance, which permits a particularly clean and direct comparison between theory and experiment and is advantageous for the study of Rydberg atoms as impurities in quantum fluids [11].

In addition, alkaline-earth metal atoms possess two active electrons, which provides new opportunities for creating and probing tailored Rydberg gases. The principal transition of the Rydberg core is typically in the visible range and can be used to drive autoionizing transitions [12], to image Rydberg atoms or ions [13], and to provide oscillator strength for magic-wavelength optical trapping of Rydberg atoms [14]. Doubly excited states serve as strong perturbers of Rydberg states, creating a much richer assortment of electronic configurations than found in alkali-metal atoms. The existence of triplet and singlet excited levels provides many Rydberg series, giving access to attractive and repulsive interactions [15]. Two-photon excitation to triplet Rydberg levels via the intermediate $^3P_1$ state, as used here, can also reduce the overall decoherence from light scattering for a given strength of optical coupling to the Rydberg level compared to the two-photon transitions available in alkali-metal atoms [16]. The results reported here represent the first experiments involving ultracold Rydberg atoms excited via intermediate triplet excited states.

Within the framework of a two-active-electron approximation, one of the two valence electrons can be excited to a Rydberg state. The interaction between the excited Rydberg electron and a neighboring ground-state atom can be described using the Fermi pseudopotential [17,18]

$$V_{\rm pseudo}(\mathbf{r}_1,\mathbf{r}_2,\mathbf{R}) = \sum_{i=1}^{2} \frac{2\pi\hbar^2 A_s[k(\mathbf{R})]}{m_e}\delta(\mathbf{r}_i-\mathbf{R}) + \frac{6\pi\hbar^2 A_p^3[k(\mathbf{R})]}{m_e}\overleftarrow{\nabla}\delta(\mathbf{r}_i-\mathbf{R})\overrightarrow{\nabla}, \quad (1)$$

where $\mathbf{r}_i$ and $\mathbf{R}$ specify the positions of the Rydberg-atom valence electron and ground-state atom, respectively, measured from the Rydberg core. The momentum-dependent s-wave and p-wave scattering lengths are $A_s(k)$ and $A_p(k)$. The Rydberg-electron momentum in a semiclassical approximation is $\hbar k(\mathbf{r}) = \sqrt{2m_e(e^2/(4\pi\varepsilon_0\mathbf{r}) - E_b)}$, where E_b is the binding energy of the unperturbed Rydberg atom. This approximation is justified for highly excited $^3S_1$ Rydberg states for which the hydrogenic approximation is valid at large r. Since only one of the two valence electrons interacts strongly with the ground-state atom, the molecular potential can be calculated using effective one-electron wave functions. The electron-electron interaction contributes to the quantum defect affecting the large-r behavior of the wave function. When the molecular potential forms an attractive well, ground-state atoms can be bound to a Rydberg atom, yielding a Rydberg molecule.

The creation of ultra-long-range molecules requires ultracold temperatures so that thermal energies that are lower than the small binding energies (~10 MHz). Also, high-density

*Corresponding author: killian@rice.edu

samples are necessary to ensure a sizable probability of finding two atoms with separations less than the radial extent of a Rydberg electronic wave function. We obtain these conditions using ^{84}Sr atoms in an optical dipole trap (ODT). This isotope has collisional properties favorable for evaporative cooling and the creation of high-phase-space-density samples [19]. Details of the cooling and trapping are given in Ref. [20].

At the start of the excitation time, the atoms are held in a pancake-shaped ODT formed by two crossed 1064-nm laser beams, both having horizontal and vertical waists of about 370 and 40 μm, respectively. The trap oscillation frequencies are 12 and 158 Hz. Typically 7×10^5 atoms are trapped at a temperature of $\sim$200 nK, yielding a peak density of $\rho = 2.7 \times 10^{12}$ cm^{-3}. This corresponds to an average interparticle spacing of $1/\rho^{1/3} = 0.7$ μm, which is about 10$\times$ the distance from the nucleus to the outer lobe of the Rydberg electron wave function, $2n^{*2}a_0 \simeq 75$ nm, for $n = 30$ and $n^* = n - \delta$. We determine the $5sns$ $^3S_1$ state quantum defect $\delta = 3.372 \pm 0.001$ by fitting observed Rydberg lines for $n = 24$ to 36, and this value agrees well with the value $\delta = 3.371$ from Ref. [15].

Atoms are promoted to Rydberg states through two-photon $5s^2$ $^1S_0$–$5s5p$ $^3P_1$–$5sns$ $^3S_1$ excitation. The 689-nm laser for the first step is detuned 170 MHz to the blue of the intermediate state to avoid scattering from the atomic line and associated molecular resonances. Rydberg states with $n = 29$–36 are reached with photons at 319 nm generated by frequency doubling the red output of a fiber-based optical parametric oscillator laser. Approximately 200 mW of UV power is available. The intensities of the red and UV light on the atoms are 2.2×10^3 and 2.3×10^5 W/m^2, respectively. The UV and 689-nm lasers copropagate with orthogonal linear polarizations. This configuration excites a superposition of $m = +1$ and $m = -1$ $^3S_1$ Rydberg states.

The frequency of the UV light is controlled by locking the 638-nm fundamental to an optical cavity stabilized to the 689-nm laser, which is locked to the $5s^2$ $^1S_0$–$5s5p$ $^3P_1$ atomic transition. The UV frequency is scanned using an acousto-optic modulator in the path of the 638-nm light en route to the stabilization cavity. The excitation time is precisely controlled using an acousto-optic modulator on the 689-nm beam, while the UV light is controlled by a slower mechanical shutter. After excitation, the atoms are released from the trap and the ground-state atom population is measured with time-of-flight absorption imaging on the $5s^2$ $^1S_0$–$5s5p$ $^1P_1$ transition at 461 nm. Excitation to atomic Rydberg or molecular levels is detected as ground-state atom loss. The exposure time is held constant for the molecular spectrum for a given quantum number and is approximately $\sim$2 s. This results in approximately 50% peak loss for excitation to the most deeply bound molecular level. For atomic resonances (data not shown), 50% peak loss is obtained for $\sim$10-ms excitation. The ODT is left on during excitation, and we assume the ac Stark shift is the same for the atomic and molecular transitions in our quoted results.

The atom-loss spectra (Fig. 1) are relatively simple because of the closed-shell $^1S_0$ electronic ground state and lack of nuclear spin for ^{84}Sr. Atom loss is an indirect method of detecting excitation compared to the traditional technique of pulsed-field ionization and charged-particle detection [2,4–7,9], but it yields a high signal-to-noise ratio. A comprehensive understanding of the decay channels of ultra-long-range molecules is still lacking, but a large fraction of excitations should lead to measurable ground-state atom loss. Fluorescent decay after either atomic or molecular excitation has an approximately two-thirds probability of creating long-lived $^3P_0$ or $^3P_2$ atoms. Such atoms may remain trapped but they are invisible to absorption imaging. The recoil energies of $h^2/2m_{84}\lambda_{689}^2 k_B = 0.24$ μK and $h^2/2m_{84}\lambda_{320}^2 k_B = 1.1$ μK are smaller than the 1.9-μK depth of the ODT. However, collisional processes involving ground-state atoms and tunneling to small internuclear separation can reduce the molecular lifetime significantly compared to the atomic lifetime for conditions similar to ours [10]. Such tunneling should release enough energy to eject one or both atoms from the trap. For atomic excitation, it is possible that the density of Rydberg atoms becomes high enough for inelastic Rydberg-Rydberg collisions to lead to atom loss [21]. The density of molecules, however, is low enough that such processes are negligible.

The threshold for the molecular-binding energy for each principal quantum number is determined by measuring the resonance position for atomic excitation to the $5sns$ $^3S_1$ state. This is done with a 10-ms excitation time to avoid saturating the transition, and it results in an $\sim$800-kHz FWHM linewidth, which is likely limited by the UV laser linewidth. For such short excitation times, no molecular transitions are visible. For excitation times of the order of 1 s, however, clearly resolved resonances corresponding to molecular bound states appear to the red of the (highly saturated) atomic line. No transitions are observed to the blue or farther to the red of the regions shown. Data are fit to the wing of a Lorentzian to describe the atomic background plus a Gaussian for each molecular line. Molecular-binding energies are determined by the frequency difference between molecular and atomic lines.

Typical molecular linewidths are 800-kHz FWHM, limited by the laser linewidth. Several spectra were recorded for each principal quantum number, alternating between measurement of atomic and molecular lines. The uncertainties in the molecular line positions with respect to the atomic line are the statistical 1σ uncertainties in the mean for each group of measurements. The typical value is $\pm$150 kHz. The dc Stark shifts of the transitions were measured for $n = 36$ by applying electric fields of up to about 0.5 V/cm. Extracted atomic and molecular dc polarizabilities were equal at our level of precision, ± 0.5 MHz/(V/cm)^2. Theoretical calculation predicts a dc polarizability of -4.5 MHz/(V/cm)^2.

For the present range of n and our relatively low densities, the production rate for trimers is expected to be much lower than for dimers [9,22] and therefore difficult to detect with our current methods. The most deeply bound level observed for each principal quantum number is assigned to the vibrational ground state of one atom in the potential well formed by the outermost lobe of the Rydberg electron wave function. This is confirmed by calculations of the potentials and molecular wave functions [Figs. 1(b), 1(d), and 1(f)], which show that this state is well localized in this well. More weakly bound levels correspond to vibrationally excited states, which are delocalized across several lobes of the electron probability density.

The electron wave function $\Psi(\mathbf{r}_1,\mathbf{r}_2)$ of the $^3S_1$ Rydberg atom can be calculated by numerically diagonalizing the Hamiltonian within the two-active-electron model. Spin-orbit

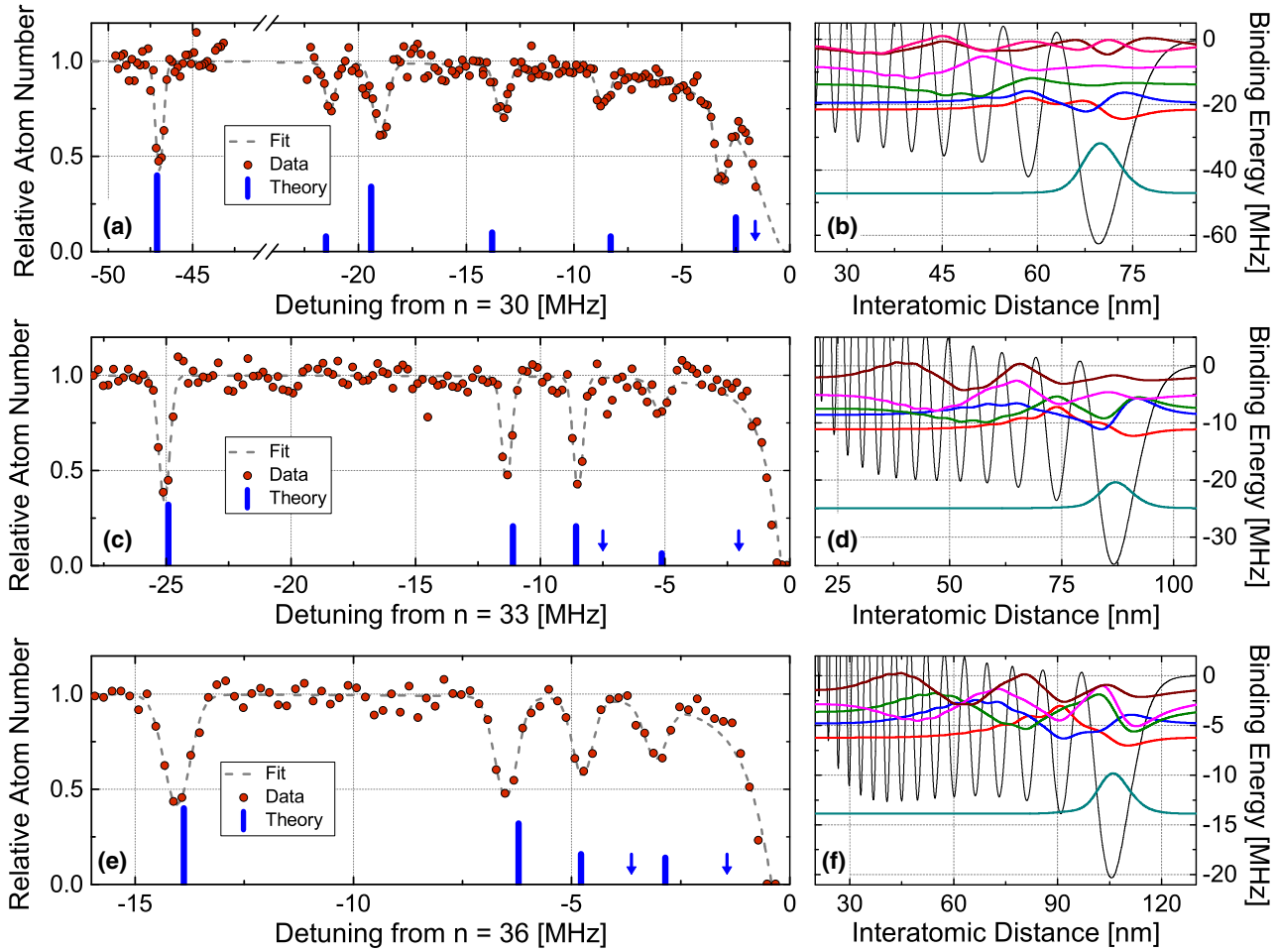

FIG. 1. (Color online) (a, c, e) Atom-loss spectra and (b, d, f) calculated potentials and wave functions, $R\chi_\nu(R)$, for $n = 30$ (a, b), $n = 33$ (c, d), and $n = 36$ (e, f). The bars at the bottom of each loss spectrum indicate the theoretically predicted binding energies of states bound by >1 MHz, with heights corresponding to their calculated excitation strengths, Γ_ν. Arrows mark the positions of additional bound states of negligible strength. The origin of each frequency axis is set to the center of the atomic excitation spectrum (see text).

interaction is included, but its effects are small [23]. The model potential is fitted to reproduce the measured energy levels in the singlet sector [24] and yields the quantum defect $\delta = 3.376$ for $^3S_1$ states, which agrees well with the more precise measured value. The calculated wave functions for $^3S_1$ Rydberg states with $n \sim 30$ are dominated by a single configuration,

$$\Psi(\mathbf{r}_1,\mathbf{r}_2) \simeq \frac{1}{\sqrt{2}}(\phi_{5s}(\mathbf{r}_1)\psi_{ns}(\mathbf{r}_2) - \psi_{ns}(\mathbf{r}_1)\phi_{5s}(\mathbf{r}_2)), \qquad (2)$$

where $\phi_{5s}(\mathbf{r})$ and $\psi_{ns}(\mathbf{r})$ are the wave functions of the $5s$ state for Sr^+ ions and the Rydberg ns state for Sr atoms, respectively. The contributions from the other configurations are less than 0.01%. Using the first-order perturbative approximation the molecular potential around $R \simeq 1000$ a.u. can be evaluated:

$$V(R) \simeq \frac{2\pi\hbar^2 A_s(k)}{m_e}|\psi_{ns}(\mathbf{R})|^2 + \frac{6\pi\hbar^2 A_p^3(k)}{m_e}|\nabla\psi_{ns}(\mathbf{R})|^2 . \qquad (3)$$

Since the second valence electron is rather localized [i.e., $\phi_{5s}(\mathbf{r}) \simeq 0$ for $r > 20$ a.u.], it does not affect the molecular potential at large R, and therefore, $V(R)$ becomes similar to that for effective one-electron systems.

By solving the Schrödinger equation associated with the molecular potential, the binding energies and the wave functions for Rydberg molecules are obtained. The effective scattering lengths are taken to be

$$A_s(k) = A_s(k=0) + \frac{\pi}{3}\alpha k, \quad A_p(k) = A_p(k=0). \qquad (4)$$

The measured value, $\alpha = 186a_0^3$, is used for the polarizability [25]. It is known [22] that a nonperturbative Green's function calculation correctly reproduces the measured molecular energy levels using the true zero-energy s- and p-wave scattering lengths. Within the first-order perturbative approximation, however, good agreement can be obtained by considering the scattering lengths as effective fitting parameters. For strontium, while the calculated s-wave scattering length is $A_s(k=0) = -18\,a_0$ [26], an effective scattering length of $A_s(k=0) = -13.2a_0$ for $n = 30$ to $A_s(k=0) = -13.3a_0$ for $n = 36$ yields good agreement with the measured energy levels, especially the most deeply bound molecular states. The depth of the deepest well in the molecular potential scales

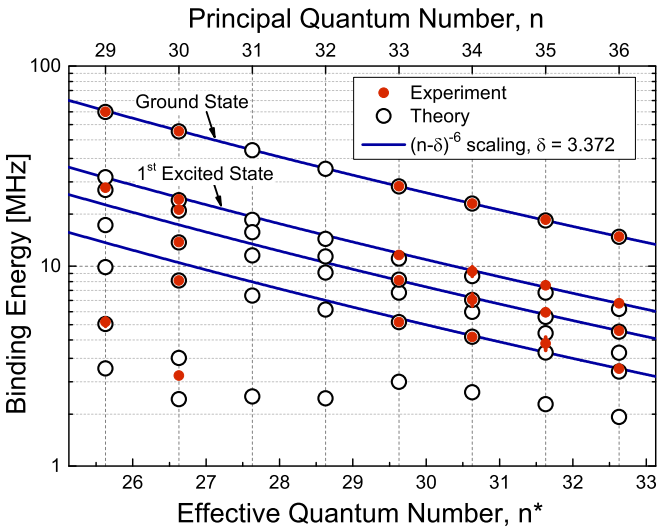

FIG. 2. (Color online) Scaling of observed molecular binding energies, showing $1/(n-\delta)^6$ scaling for higher quantum numbers and more deeply bound levels.

linearly with $A_s(k=0)$ [Eq. (3)]. The additional contribution from p-wave scattering becomes non-negligible around the nodes (i.e., $|\psi_{ns}(\mathbf{R})| \simeq 0$) and affects the energies and density of states for the weakly bound levels. $A_p(k=0) \simeq 8.4a_0$ yields an optimal fit.

The molecular formation rate can be estimated as $\Gamma_\nu \propto |\langle \Psi, \chi_\nu | T | \Psi_0, \chi_0 \rangle|^2$, where T is the transition matrix for two-photon absorption, and Ψ_0, χ_0, and χ_ν are the ground-state-electron wave function, the initial state, and the νth vibrational wave function of the Rydberg molecule, respectively. Within first-order perturbation theory, the electronic part of the transition matrix is independent of the molecular states. Therefore, the excitation rate is reduced to the Franck-Condon factor:

$$\Gamma_\nu \propto \left| \int dR\, R^2\, \chi_\nu(R) \chi_0(R) \right|^2 . \tag{5}$$

In the present case χ_0 can be approximated as the square root of the pair distribution of two unbound ground-state Sr atoms, which is approximately constant for the large-R values contributing to the integral [Eq. (5)]. The vertical bars in Fig. 1 denote the positions of the calculated energy levels, with heights corresponding to the excitation rates, Γ_ν. The calculated rates are in reasonable accord with the strength of the corresponding loss features. The calculations reveal the existence of additional molecular levels with excitation strengths too weak to be detected.

Figure 2 shows the n scaling of observed and calculated values for binding energies. Gaps in laser coverage prevented measurement of spectra for $n = 31$ and $n = 32$. The binding energies of deeply bound states follow the approximate $1/(n-\delta)^6$ scaling initially seen in Rb [9], which reflects the scaling of the Rydberg-electron probability density $|\psi_{ns}(\mathbf{R})|^2$ at the location of the ground-state Sr atom. Deviations from the scaling are evident for weakly bound states and are clearly seen in high-quality spectra for $n = 30$. These deviations occur, for example, when the first excited state of the outer potential well is nearly degenerate with the lowest energy state of the adjacent well. Tunneling between the wells produces a coupling and energy splitting for the two states and a deviation from the $1/(n-\delta)^6$ scaling.

We have presented the first observation of ultra-long-range Rydberg molecules in Sr_2 formed by photoexcitation to the $5sns\ ^3S_1$ Rydberg state for $29 \leqslant n \leqslant 36$. The observed lines are well described using a Fermi pseudopotential approach to calculate perturbative molecular potentials and yield the effective s-wave and p-wave e^--Sr scattering lengths $A_s = -13.2a_0$ and $A_p = 8.4a_0$.

This work represents the first study of ultra-long-range Rydberg molecules in a divalent atomic system. It opens new opportunities for particularly detailed comparisons between theory and experiment without the complexities associated with alkali-metal Rydberg molecules, and it enables new directions in this emerging research area. For example, doubly excited electronic states give rise to dramatic perturbations of the Rydberg states in divalent atoms. This should lead to new types of ultra-long-range molecules with mixed electronic character that arise from degeneracies of pairs of Rydberg levels of different angular momenta. This may also lead to very high transition strengths for production of molecules with large dipole moments. If one can form Rydberg molecules with high electronic angular momenta, it might be possible to optically trap them using the oscillator strength of the ionic core [14]. High densities of atoms in metastable triplet levels can be created in these systems [27], allowing the formation of Rydberg molecules in which triplet atoms serve as the "ground-state" atoms. Spectroscopy of these molecules will probe the low-energy scattering of electrons from the metastable states including measurement of the electron-triplet scattering length, which should be sensitive to the greater polarizability compared to closed-shell, ground-state atoms.

Detection of ultra-long-range molecules with atom loss, as demonstrated here, greatly simplifies the required experimental apparatus compared to charged particle detection, which may open the way for study of these exotic molecules in many other species of atomic gases. The measurements reported here also represent an important step towards future experiments with interacting alkaline-earth Rydberg atoms because molecular excitations represent loss channels that need to be avoided.

This research was supported by the AFOSR under Grant No. FA9550-14-1-0007, the NSF under Grants No. 1301773 and No. 1205946, the Robert A. Welch Foundation under Grants No. C-0734 and No. C-1844, the FWF (Austria) under Grant No. P23359-N16, and FWF-SFB049 NextLite. The Vienna Scientific Cluster was used for the calculations.

[1] C. H. Greene, A. S. Dickinson, and H. R. Sadeghpour, Phys. Rev. Lett. **85**, 2458 (2000).

[2] V. Bendkowsky, B. Butscher, J. Nipper, J. P. Shaffer, R. Löw, and T. Pfau, Nature **458**, 1005 (2009).

[3] W. Li, T. Pohl, J. M. Rost, S. T. Rittenhouse, H. R. Sadeghpour, J. Nipper, B. Butscher, J. B. Balewski, V. Bendkowsky, R. Löw *et al.*, Science **334**, 1110 (2011).
[4] J. Tallant, S. T. Rittenhouse, D. Booth, H. R. Sadeghpour, and J. P. Shaffer, Phys. Rev. Lett. **109**, 173202 (2012).
[5] M. A. Bellos, R. Carollo, J. Banerjee, E. E. Eyler, P. L. Gould, and W. C. Stwalley, Phys. Rev. Lett. **111**, 053001 (2013).
[6] H. Saßmannshausen, F. Merkt, and J. Deiglmayr, Phys. Rev. Lett. **114**, 133201 (2015).
[7] A. T. Krupp, A. Gaj, J. B. Balewski, P. Ilzhöfer, S. Hofferberth, R. Löw, T. Pfau, M. Kurz, and P. Schmelcher, Phys. Rev. Lett. **112**, 143008 (2014).
[8] D. A. Anderson, S. A. Miller, and G. Raithel, Phys. Rev. Lett. **112**, 163201 (2014).
[9] A. Gaj, A. T. Krupp, J. B. Balewski, R. Löw, S. Hofferberth, and T. Pfau, Nature Commun. **5**, 4546 (2014).
[10] B. Butscher, V. Bendkowsky, J. Nipper, J. B. Balewski, L. Kukota, R. Löw, T. Pfau, W. Li, T. Pohl, and J. M. Rost, J. Phys. B **44**, 184004 (2011).
[11] J. B. Balewski, A. T. Krupp, A. Gaj, D. Peter, H. P. Büchler, R. Lowe, S. Hofferberth, and T. Pfau, Nature **502**, 664 (2013).
[12] J. Millen, G. Lochead, and M. P. A. Jones, Phys. Rev. Lett. **105**, 213004 (2010).
[13] P. McQuillen, X. Zhang, T. Strickler, F. B. Dunning, and T. C. Killian, Phys. Rev. A **87**, 013407 (2013).
[14] R. Mukherjee, J. Millen, R. Nath, M. P. A. Jones, and T. Pohl, J. Phys. B **44**, 184010 (2011).
[15] C. L. Vaillant, M. P. A. Jones, and R. M. Potvliege, J. Phys. B **45**, 135004 (2012).
[16] N. Henkel, R. Nath, and T. Pohl, Phys. Rev. Lett. **104**, 195302 (2010).
[17] E. Fermi, Nuovo Cimento **11**, 157 (1934).
[18] A. Omont, J. Physique **38**, 1343 (1977).
[19] Y. N. Martinez de Escobar, P. G. Mickelson, P. Pellegrini, S. B. Nagel, A. Traverso, M. Yan, R. Côté, and T. C. Killian, Phys. Rev. A **78**, 062708 (2008).
[20] Y. N. Martinez de Escobar, P. G. Mickelson, M. Yan, B. J. DeSalvo, S. B. Nagel, and T. C. Killian, Phys. Rev. Lett. **103**, 200402 (2009).
[21] F. Robicheaux, J. Phys. B **38**, S333 (2005).
[22] V. Bendkowsky, B. Butscher, J. Nipper, J. B. Balewski, J. P. Shaffer, R. Löw, T. Pfau, W. Li, J. Stanojevic, T. Pohl *et al.*, Phys. Rev. Lett. **105**, 163201 (2010).
[23] C. L. Vaillant, M. P. A. Jones, and R. M. Potvliege, J. Phys. B **47**, 155001 (2014).
[24] S. Ye, X. Zhang, F. B. Dunning, S. Yoshida, M. Hiller, and J. Burgdörfer, Phys. Rev. A **90**, 013401 (2014).
[25] H. L. Schwartz, T. M. Miller, and B. Bederson, Phys. Rev. A **10**, 1924 (1974).
[26] K. Bartschat and H. R. Sadeghpour, J. Phys. B **36**, L9 (2003).
[27] A. Traverso, R. Chakraborty, Y. N. Martinez de Escobar, P. G. Mickelson, S. B. Nagel, M. Yan, and T. C. Killian, Phys. Rev. A **79**, 060702(R) (2009).